



# CXCL10 Produced by HPV-Positive Cervical Cancer Cells Stimulates Exosomal PDL1 Expression by Fibroblasts *via* CXCR3 and JAK-STAT Pathways

OPEN ACCESS

Xiaona Chen<sup>1,2†</sup>, Hui He<sup>3†</sup>, Yue Xiao<sup>1,2</sup>, Ayshamgul Hasim<sup>4</sup>, Jianlin Yuan<sup>5</sup>, Min Ye<sup>6</sup>, Xin Li<sup>1,2\*</sup>, Yi Hao<sup>7\*</sup> and Xia Guo<sup>1,2\*</sup>

**Edited by:**

Dayanidhi Raman,  
University of Toledo, United States

**Reviewed by:**

Janin Chandra,  
University of Queensland, Australia  
Fenfen Wang,  
Zhejiang University, China  
Enrique Boccardo,  
University of São Paulo, Brazil

**\*Correspondence:**

Xia Guo  
guoxia0504\_sz@163.com  
Yi Hao  
haoyi0320sz@163.com  
Xin Li  
xinli268@gmail.com

<sup>†</sup>These authors have contributed  
equally to this work

**Specialty section:**

This article was submitted to  
Women's Cancer,  
a section of the journal  
Frontiers in Oncology

**Received:** 14 November 2020

**Accepted:** 26 May 2021

**Published:** 06 August 2021

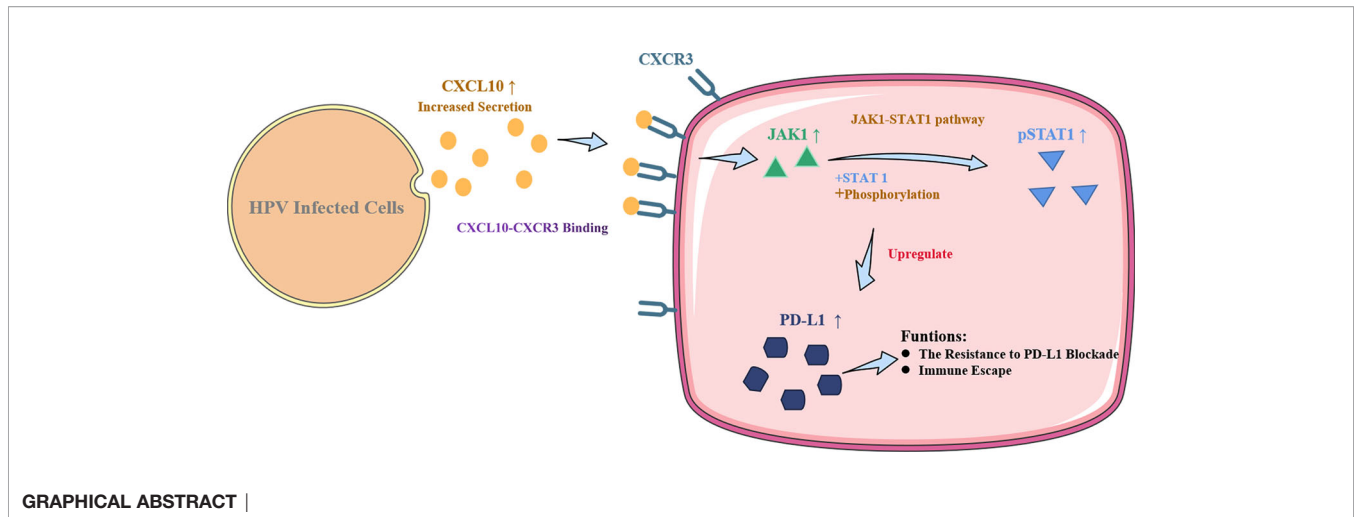
**Citation:**

Chen X, He H, Xiao Y, Hasim A,  
Yuan J, Ye M, Li X, Hao Y and  
Guo X (2021) CXCL10 Produced  
by HPV-Positive Cervical Cancer  
Cells Stimulates Exosomal PDL1  
Expression by Fibroblasts *via*  
CXCR3 and JAK-STAT Pathways.  
*Front. Oncol.* 11:629350.  
doi: 10.3389/fonc.2021.629350

<sup>1</sup> Center for Clinical Research and Innovation (CCRI), Shenzhen Hospital, Southern Medical University, The Third School of Clinical Medicine, Southern Medical University, Shenzhen, China, <sup>2</sup> Clinical Medical Research Center, Shenzhen Hospital, Southern Medical University, Shenzhen, China, <sup>3</sup> Department of Pathology, Shenzhen Hospital, The University of Hong Kong, Shenzhen, China, <sup>4</sup> Department of Pathology, Basic College, Xinjiang Medical University, Urumqi, China, <sup>5</sup> Department of Gynecology, Affiliated Cancer Hospital, Xinjiang Medical University, Urumqi, China, <sup>6</sup> Department of Pathology, Affiliated Cancer Hospital, Xinjiang Medical University, Urumqi, China, <sup>7</sup> Department of Ultrasound, South China Hospital of Shenzhen University, Shenzhen, China

Persistent infection with human papillomavirus (HPV) and immune surveillance failure may be the initiating factors for the carcinogenesis of cervical squamous cell carcinoma (CSCC). HPV infection might affect the innate immune pathway of cervical epithelial cells that constitute the “microenvironment” for tumor cells. Programmed death-ligand 1 (PD-L1) has been reported to be an immunosuppressor that helps cancer cells escape the actions of T cells. In the present study, CXCL10 was substantially upregulated both in cervical tissues of HPV infected patients with cervical intraepithelial neoplasia (CIN) or CSCC, as well as in HPV16 E6/E7 transgenic murine cervix. The HPV-positive (HPV+) cervical cancer cell lines SiHa and Caski secreted increased levels of CXCL10 compared to human foreskin fibroblasts (HFF-1), and its receptor CXCR3 was overexpressed in HFF-1. After co-culture with SiHa or Caski, the JAK-STAT signaling pathway and exosomal PD-L1 expression were both upregulated in HFF-1. Recombinant human CXCL10 induced JAK-STAT and PD-L1, while the CXCL10-CXCR3 and JAK-STAT inhibitors AMG487 or ruxolitinib reduced the expression of PD-L1 in HFF-1 cells. Furthermore, the upregulated expression of PD-L1 was verified in HPV+ but not HPV-negative (HPV-) patients with cervical cancers by analysis of tissue microarray cores in 25 cervical lesion patients ( $P < 0.05$ ). The results indicate that HPV infection can induce cervical cancer cells to secrete CXCL10, which binds to CXCR3 in the surrounding fibroblast cells, leading to JAK-STAT pathway activation and the subsequent upregulated expression of exosomal PD-L1. These mechanisms may help HPV to escape immune response attack, leading to carcinogenesis.

**Keywords:** human papillary virus, CXCL10-CXCR3 axis, innate and adaptive immune responses pathways, TLR signaling pathways, PD-L1, cervical cancer, JAK-STAT



## INTRODUCTION

Cervical cancer is the second most common malignancy in women after breast cancer, and a high-risk of human papillomavirus (hrHPV) infection is the primary cause (1, 2). While most HPV infections can be cleared by the human immune system, a small subset of persistent infections develop from cervical intraepithelial neoplasia I (CINI) that progresses to CIN III and then invasive carcinoma (3, 4). Therefore, persistent infection with hrHPV and immune surveillance failure may be the initiating factors for cervical cancer. The HPV E6 and E7 oncogenes (5), key factors in viral carcinogenesis, are capable of causing malignant transformation by targeting the critical tumor suppressors p53 and pRb, which are effectively the “Achilles heel” of genomic stability (6, 7). However, less is known about how HPV genes help HPV-infected cells to evade immune responses (8, 9). Viruses have developed powerful immunosuppressive mechanisms including targeting antigen processing and presentation, which are the processes required for effective innate and adaptive immune responses (10).

Innate immunity is the body’s first line of defense against microbial and virus invasion. Previous studies have demonstrated that signals from a virus invading cells can be recognized by sentinel receptors in the natural immune system, which in turn triggers the activation of innate immune pathways, regulate adaptive immune responses and initiate downstream signaling cascades that produce proinflammatory cytokines and chemokines (11, 12). CXC motif chemokine 10 (CXCL10), also known as interferon gamma-induced protein-10 (IP-10), is a small cytokine-like protein secreted by a wide variety of cell types. CXCL10 is a ligand of the CXC chemokine receptor-3 (CXCR3) and is predominantly expressed by T helper cells (Th cells),

cytotoxic T lymphocytes (CTLs), dendritic cells, macrophages, natural killer cells (NKs), as well as some epithelial and cancer cells (13, 14). The CXCL10/CXCR3 signaling pathway mediates paracrine interactions between tumor and stromal cells that govern leukocyte trafficking and angiogenesis. Emerging data have implicated the non-canonical CXCL10/CXCR3 axis in tumorigenesis and metastasis.

Recent research has suggested that the CXCL10/CXCR3 axis may be associated with the promotion and induction of various types of cancers including breast cancer (15, 16), pancreatic cancer (PCC) (17), hepatocellular carcinoma (HCC) (18, 19), melanoma (17), lymphoma (20), brain cancer (21), papillary thyroid carcinoma (PTC) (22), lung adenocarcinoma (23) and osteosarcoma (24). In the present study, CXCL10 expression was substantially upregulated both in cervical tissues of HPV infected patients with CIN or CSCC, as well as in hrHPV16E6/E7 transgenic mice, as determined by PCR array analysis of gene expression profiling in innate and adaptive immune response pathways; these findings suggested a pivotal role for hrHPV in driving tumorigenesis. Cytotoxic T lymphocyte dysfunction is frequently associated with activation of PD-L1/PD-1 and is a principal obstacle in opposing cancer therapy. Several studies have investigated whether HPV infection can affect PD-L1 expression in cervical cancer and found that HPV-positivity was positively correlated with increased PD-L1 expression (25). In the present study, the mechanisms underlying HPV E6/E7 induced evasion of cervical cancer cells from the host immune system *via* the CXCL10-CXCR3 axis were investigated (26).

## METHODS

### Collection of Clinical Specimens Tissue Samples

Cervical lesions tissues and matched cervical exfoliated cell specimens were collected from cervical lesion patients, including normal tissue (20 cases, NC), high grade squamous intraepithelial lesion (HSIL, including CIN II/III lesions), and

**Abbreviations:** HPV, human papilloma virus; PD-L1, Programmed death-ligand 1; CSCC, Cervical squamous-cell carcinoma; CIN, cervical intraepithelial neoplasia; HSIL, high grade squamous intraepithelial lesion; CXCL10, CXC motif chemokine 10; CXCR3, CXC chemokine receptor-3; Th cells, T helper cells; CTLs, cytotoxic T lymphocytes; NKs, natural killer cells; PC, pancreatic cancer; HCC, hepatocellular carcinoma; PTC, papillary thyroid carcinoma.

early cervical squamous cell carcinoma (staged before IIa, 20 cases, CSCC) at the Affiliated Tumor Hospital of Xinjiang Medical University with patients' agreement. These cases were selected according to clear pathological diagnoses based on the World Health Organization (27) diagnostic criteria. The patients had not previously received preoperative anticancer therapy. Informed consent was obtained from each patient enrolled and the collection of tissue specimens was approved by the Internal Review and Ethics Boards of the Affiliated Tumor Hospital of Xinjiang Medical University. Tissue microarray chips containing 90 pairs of CSCC tissue specimens, matched to adjacent non-tumoral (NT) cervical tissue specimens, and the associated clinicopathological information were purchased from Shanghai OUTDO Biotech Co. (Shanghai).

### Detection and Genotyping of HPV

The Hybrid Capture<sup>®</sup> 2 system (hc2, Digene Corp., USA) was purchased by the Cancer Hospital affiliated to Xinjiang Medical University. The second-generation hybrid capture 2 (hc2) assay is the only method currently approved for clinical hrHPV DNA testing by the US Food and Drug Administration (FDA) and the China Food and Drug Administration (CFDA). A total of 37 HPV genotypes including 16, 18, 31, 33, 35, 39, 45, 51, 52, 56, 58, 59, 66, 68, 6, 11, 42, 43, 44, 81, 53, 26, 34, 40, 54, 55, 57, 61, 67, 69, 70, 71, 72, 73, 82, 83 and 84, and multiple infections could be accurately detected with both a sensitivity and specificity > 95%. Especially, based on the guidelines used for clinical diagnosis, the method can detect 13 HR-HPV types (-16, -18, -31, -33, -35, -39, -45, -51, -52, -56, -58, -59 and -68) or 5 LR-types (-6, -11, -42, -43 and -44), as well as the HPV DNA load. The assay was a non-radioactive signal-amplification method based on the hybridization of the target HPV-DNA to labeled RNA probes in solution, utilizing signal amplification of antibody capture and detection of chemiluminescence signals in 96-well plates.

### PCR Array Analysis of Innate and Adaptive Immune Responses as Well as TLR Signaling Pathways

Two groups (HSIL, CSCC) of HPV16/18-positive patients with cervical lesions (a total of 31 cases) and the cervical tissue specimens without HPV16/18 lesions or other HPV subtypes (NC) as the controls were selected from 60 specimens previously collected. RT<sup>2</sup> profiler PCR array gene expression analysis was used for differential analysis of TLR signaling pathways (QIAGEN, Cat. no. PAHS-018Z), as well as innate and adaptive immune response pathways (84 genes) (QIAGEN, Cat. no. PAHS-052Z) (Tables S2A, B) by using the human tissue sample described above. PCR arrays were used to analyze the differential expression of receptors, virus-specific response molecules, pathway regulatory molecules, upstream and downstream effector molecules in innate and adaptive immune response, Th1, Th2, Th17, Treg marker molecules, inflammatory response and anti-viral immune response molecules. The operational steps were performed according to Qiagen's operating procedures. The protocol can be briefly described as follows:

Total RNA was extracted from tissue using a RNeasy Microarray Tissue Mini Kit and purified (RNeasy@ MinElut<sup>™</sup>, Qiagen) to ensure RNA quality. Reverse transcriptase MLV-RT was used to synthesize the cDNA using 1.0 µg of total RNA as a template. 2 x SYBR Green Fluor qPCR Master Mix was prepared according to the requirements of the assay. Subsequently, sample cDNA and MasterMix were added to 96 wells, respectively in which 84 genes, 5 housekeeping genes and 7 controls were detected. Online data analysis software was used to analyze the original CT values obtained by real-time quantitative PCR to form a scatter map, and the RNasy microarray tissue mini-kit map was grouped.

### Cell Culture

HFF-1, and Caski cells were purchased from the Cell Bank of Chinese Academy of Sciences. H8 and SiHa cells were kindly provided by Prof. Abulizi Abudula. SiHa, Caski and H8 cells were cultured in RPIM1640 media (Gibco, US) and HFF-1 cultured in DMEM (HyClone, US) supplemented with 10% fetal bovine serum (Biological Industries, Israel), and 100 U/ml penicillin/streptomycin (Biological Industries, Israel). Cells were cultured in a 5% CO<sub>2</sub> incubator at 37°C. When cultures became confluent, the cells were treated with 0.25% trypsin (Gibco, US) containing 0.02% EDTA for 2 min at room temperature.

### HPV E6/E7 Knockout by CRISPR/Cas9 Gene Editing

CRISPR/Cas9 single guide sequences specifically targeting HPV16 infection marker E6/E7 (sg E6/E7) were designed in Vector Builder ([www.vectorbuilder.com](http://www.vectorbuilder.com)) and produced by the Cyagen Company. The E6/E7 gRNA guide sequence used were 5'-CAACAGTTACTGCGACGTG-3' and 5'-TCCGGTTCTGCTGTCC AGC-3'. SiHa cell lines were transduced twice with first sgRNAE6/E7 lentiviruses, EGFP lentiviruses as the positive control and transfection reagent as the negative control. Puromycin (Merck, Germany) was added on day 4 at a minimal toxic dose to select transduced cells. Then after 3 days of screening, the condition of the cells was observed, and a second transduction performed with Cas9 lentiviruses. Hygromycin at a minimal toxic dose was added after 3 days. The second screening finished after all negative control cells had died. To minimize off-target errors, monoclonal screening was conducted. Single colonies were spread in a 96-well plate and selected by a colony formation assay. The effect of E6/E7 gene editing on cell proliferation was assessed by Trypan Blue viable cell counting over a 7-day time course. The cell apoptosis induction and proliferation inhibition of Ko E6/E7 SiHa cells were markedly induced *in vitro*, which were also cultured in RPIM1640 media (Gibco, US) containing 10% FBS in a 5% CO<sub>2</sub> incubator at 37°C. Lentiviral transduction efficiency was proven by employing RT-qPCR and western blotting techniques. Total protein from SiHa cells was extracted using RIPA buffer (Solabio, China) and protein expression was determined by western blotting, probed for E6/E7 (Abcam; ab70, ab30731), GAPDH (Yeaston, China) using sensitive ECL detection (Yeaston, China). Total RNA extraction and the methods of RT-qPCR are

described below and the E6 and E7 primers used are listed in **Table S3**.

## Transgene Construction and Production of Transgenic Mice

The diagram illustrating the vector map used to generate transgenic mice was shown in **Figure S1A**. The gene for HPV16 E6/E7 was placed under the control of the K14 promoter using standard methods. The plasmid DNA employed was purified using the method of plasmid midiprep and then used for microinjection into fertilized eggs of C57BL/6×C57BL/6 hybrid mice. The transgenic (Tg) mice were identified by PCR (Transgene PCR primer F1: TCACTCAGCCAACTGCTCGC; Transgene PCR primer R1: GTCGCAGTAACTGTTGCTTGCAG) (**Figure S1B**). Eight founder lines were established by breeding into C57BL/6×C57BL/6 hybrid mice. The line with the highest transgene expression was selected for further analysis. Most experiments were carried out using heterozygous mice that were housed and fed under specific pathogen free environment. In order to identify the phenotype of the cervix tissues, the tissues from the HPV16 E6/E7 transgenic mice were analyzed histologically. The procedures for care and use of animals were approved by the Ethics Committee of the Shenzhen Hospital of Southern Medical University and all applicable conditions according to strict institutional and governmental regulations concerning the ethical use of animals were followed.

## RNA Sequencing

Three copies of SiHa and KoE6/E7 SiHa cell specimens were dissolved in Trizol, and the RNA-seq was determined by the Novo Nordisk Company. The analysis results were evaluated with the aid of the KEGG library. After RNA extraction, the concentration and quality of the total RNA was determined using agarose gel electrophoresis and the RNA stripe was found to be complete, which indicated no degradation. The total RNA purity (OD 260/280) was detected by Nanodrop and the total RNA accurately quantified using Qubit.

## Complementary DNA Library Preparation and Sequencing

The RNA was first enriched with oligo magnetic beads, then fragmented into small pieces using a fragmentation buffer and first-strand complementary DNA was generated using a primer random template. Second-strand cDNA was synthesized by adding dNTPs and DNA polymerase I and the synthesis of cDNA was purified using AMPure XP beads. Double-stranded cDNA was repaired by adding polyA-sequencing joint. DNA fragments combined with a specifically labeled joint were amplified by PCR and the PCR system was purified using BECKMAN AMPure XP beads. After the establishment of a library, Qubit 2.0 was used for preliminary quantification and then the quality test of the library was conducted using an Agilent 2100 Bioanalyzer machine. The library was quantified by qPCR to ensure its quality and finally HiSeq/MiSeq sequencing for the qualified library was completed. After the quality assessment of the original sequencing data, GO analysis, KEGG enrichment

pathway and a protein interaction network were used to analyze the levels and expression of differential proteins.

## Tissue Microarray

Tissue microarrays were obtained from Outdo Biotech Co., Ltd. (Shanghai, People's Republic of China). IHC studies of PD-L1 were performed on cervical cancer and normal specimens of tissue in a microarray using anti-PD-L1 antibodies (Proteintech). Quantitative analysis of the staining was conducted based on the percentage of positive cells and staining density by three experienced pathologists. For data analysis, staining scores < 2 were defined as low expression and scores > 2 as high expression.

## Immunohistochemistry and HE Staining

After tissues had been collected and fixed, they were typically dehydrated and embedded in melted paraffin wax, and finally cut into thin slices. The slices were affixed to microscope slides at which point the wax was removed with a solvent and the tissue slices were rehydrated. Arrays were dewaxed and then doused with endogenous peroxidase 3% hydrogen peroxide. Followed by blocking using PBS supplemented with 10% goat serum at 30mins, the specific antibody, E6 (Bioss,bs-1719R) and E7 (Bioss, bs-4623R),were incubated at 4°C overnight, and the secondary antibody was incubated at room temperature for 30 min. Cells were washed with PBS, and then incubated with the appropriate secondary antibody for 30 min at room temperature. Then DAB was added for 10 min incubation and cells were finally stained with hematoxylin. Cells were viewed and photographed using a microscope.

## Total RNA Isolation and Quantitative Real-Time PCR

Total RNA was isolated using TRIzol reagent (Invitrogen, US) and cDNA was generated using the Hifair<sup>®</sup> II 1st Strand cDNA Synthesis SuperMix (Yeason, China). qPCR was performed using a 7500 system (ABI, USA) with Hieff qPCR SYBR Green Master Mix (Yeason, China). The relative expression levels of the target genes were normalized to the expression level of the internal control GAPDH. The data analyses were performed using the  $2^{-\Delta\Delta Ct}$  method and the primer sequences are listed in **Supplementary Table 3 (Table S3)**.

## Western Blotting

Cultured cells were lysed with lysis buffer. Equal amounts of protein were run on 10% SDS-PAGE and electrotransferred to polyvinylidene fluoride membranes (Millipore). After blocking with 5% milk in TBST, membranes were incubated with primary antibodies overnight. The following antibodies were used: anti-HPVE6 (1:1000, Arigo), anti-HPVE7(1:1000, Bioss), (anti-CXCL10 (1:1,000, Abcam), anti-CXCR3 (1:1,000, Boster), anti-PDL1 (1:2,000, proteintech), anti-STAT1 (1:1,000, proteintech), anti-pSTAT1 (1:1,000, Abcam), anti-JAK1 (1:2,000, proteintech), anti-GAPDH (1:6,000, Yeasen) and anti-tublin (1:3,000, Yeasen). Membranes were then incubated with the rabbit peroxidase-conjugated secondary antibody (1:10,000, Abclonal). The blots were detected by sensitive chemiluminescence

liquid analysis (Yeasen) and Biorad software was used to capture the images.

## siRNA Transfection

The siRNA transfection referred to Ribo Company transfection guidance, and the target sequence of HPV6 siRNA was GTAGAGAAACCCAGCTGTA. 12 – 16 h prior to transfection,  $2 \times 10^5$  cells per well were planted on 24-well culture plates. Then a mixture of buffer, siRNA and reagent was prepared and incubated at room temperature for 15 min before being added to cells. After 36 – 48 h post-transfection, the cells were further collected in lysis buffer for western blot analysis.

## Transwell Co-Culture Assay

For transwell co-culture assay, 0.4  $\mu\text{m}$  PC transwell (Corning) was used to do this experiment. The SiHa or Caski cells were planted in upper chamber at a density of  $2\text{--}3 \times 10^5$  cells per well and HFF-1 or Ko E6/E7 SiHa cells were planted in the lower chamber at a density of  $2 \times 10^5$  cells per well. When all cells were adherent, the cells in the upper chamber and lower chamber were co-cultured together for 48 h through transwell assay. Furthermore, the CXCL10 (AMG487, MCE) (26) and JAK1-STAT1 (Ruxonitilib, MCE) inhibitor (28) were added into the upper chamber at a concentration of 1  $\mu\text{M}$  for 12 h treatment. And Recombinant Human CXCL10 (Novoprotein, CX32) were added to the culture media directly at a concentration of 100 ng/ml for 48 h.

## ELISA

Rat IP-10/CXCL10 (Interferon Gamma Induced Protein 10 kDa) ELISA Kit (Elabscience) analysis was performed according to manufacturer's instructions. For detection of PD-L1 on extracellular vesicles, cell supernatants, 100  $\mu\text{l}$  of extracellular vesicle samples purified from cell culture supernatants, were added to ELISA plates (96-well) (Elabscience) and left to incubate for 1 h and then 100  $\mu\text{L}$  of Biotinylated Detection Ab Diluent against PD-L1 was added and allowed to incubate for 1 h at 37°C. After discarding the liquid in the plate, 100  $\mu\text{L}$  of HRP conjugate was added to each well for a 0.5 h incubation time at 37°C and then 90  $\mu\text{L}$  of substrate was added to each well for 15 min. Plates were stopped with 50  $\mu\text{L}$  of stop solution. The plates were read at 450 nm on a BioTek plate reader and the concentration of ip-10/CXCL10 was in direct proportion to the OD 450 value. The concentration of ip-10/CXCL10 in a sample was calculated against a standard curve.

## Proliferation Assay

For CCK8 assay, the cells were plated at a density of 3,000 cells per well in 96-well plates. After adhesion to wall, 10  $\mu\text{l}$  CCK8 was added into the 100  $\mu\text{l}$  cell culture medium and the cells were incubated for 2 h at 37°C. Then cell viability was determined at a 570 nm wavelength using the CCK-8 assay according to the manufacturer's instructions (Meilunbio, MA0218-3) (**Figure S3A**).

## Apoptosis Analysis

Apoptosis was assessed by Annexin V staining and flow cytometry analysis. Briefly,  $5 \times 10^5$  SiHa or KoE6/E7 SiHa cells

were harvested, washed in PBS, and then analyzed by Annexin V/propidium iodide staining by flow cytometry according to the manufacturer's protocol (Annexin V-APC PI kit; Biolegend) (**Figure S3B**).

## Subcutaneous Tumor Formation Studies

The tumor model was established by subcutaneous (s.c.) injection of  $5 \times 10^5$  SiHa or KoE6/E7 SiHa cells in 120  $\mu\text{l}$  PBS into the flank of nude mice. Tumor volumes were determined from caliper measurements of tumor length (L) and width (W) according to the formula  $L \times W^2/2$ . Both tumor size and body weight were measured 3 times each week (**Figure S3C**). At the end of the experiment, tumors were removed and fixed in 4% paraformaldehyde, then the structure of the tissue was determined by means of HE staining and immunohistochemistry (**Figures S3D, E**).

## Purification of Extracellular Vesicles

For exosome purification from cell culture supernatants, cells were cultured in media supplemented with 10% exosome depleted FBS. Supernatants were collected from 48 – 72 h cell cultures and the extracellular vesicles were purified by a standard differential centrifugation protocol (29). In brief, culture supernatants were centrifuged at 2,000 g for 20 min to remove cell debris and dead cells (Beckman Coulter, Allegra X-14R). Microvesicles were pelleted after centrifugation at 10,000g for 30 min (Beckman Coulter, J2-HS) and resuspended in PBS. Supernatants were then centrifuged at 100,000 g for 2 h at 4°C (Beckman Coulter, Optima XPN-100) to collect exosomes and then 100,000 g centrifugation for 2 h was repeated and exosomes washed. The exosomes were dissolved in PBS and stored at -20°C or -80°C.

In addition, approximately 1 ml blood was collected from the heart of mice in order to obtain exosomes from per mouse, using anticoagulation tubes to prevent blood clotting in 17<sup>th</sup> day after subcutaneous (s.c.) injection. Immediately, the blood was centrifuged at 3,000 rpm for 10 min to remove blood cells, then the upper layer of plasma was gently aspirated, and this procedure was repeated twice. The collected plasma was centrifuged at 10,000 g for 30 min to remove extracellular macrovesicles, then the supernatant was filtered through a 0.22  $\mu\text{m}$  filter and finally centrifuged at 120,000 g for 90 min using an ultra-high speed centrifuge to remove the supernatant. The precipitate was then resuspended with PBS and centrifuged at 120,000 g for 90 min and then supernatant was carefully removed. The precipitate was resuspended with PBS which actually were the exosomes and stored at -80°C.

## Statistical Analysis

$C_T$  values were exported to an Excel file to create a table of  $C_T$  values. This table was then uploaded to the data analysis web portal at <http://www.qiagen.com/qiageneglobe>. Specimens were assigned to control or test groups.  $C_T$  values were normalized based on manual selection of reference genes. Statistical evaluations were also conducted using Graphpad Prism (version 7.0) and IBM SPSS software (version 24.0). The Shapiro-Wilk W test was used to determine whether data were

normally distributed continuous variables. Levene's test was used to justify equality of variances. A *t*-test was used to analyze mean values for normally distributed continuous variables and a Mann-Whitney U test to compare mean values for non-normally distributed continuous variables. Correlations between relative mRNA expression and quantitative titer for HPV infection were evaluated by Spearman's correlation. For all statistical tests, a *P*-value < 0.05 (two-tailed test) was considered to be a statistically significant finding.

## RESULTS

### hrHPV Infection in Different Cervical Lesion Progressions

For 60 specimens constituting 20 each for the normal cervix (NC, A group), HSIL (B group) and CSCC (C group) groups, HPV positive infections were detected in 2, 17 and 20 cases respectively, with high-risk HPV infections in 0, 14 and 17 cases, and low-risk HPV infections in 2, 3 and 3 cases (Table 1). The distribution of hrHPV infections in different types of cervical lesions in Xinjiang (n%) were: no hrHPV infections found in 20 patients in the NC group; in the HSIL group, hrHPV infection was primarily HPV16 (40%), HPV52 (20%), and HPV31 (15%); the infection rate of HPV16 was significantly higher than in the normal control group (*P* < 0.05) (Table 2).

### Identification of Upregulated Expression of CXCL10 in HPV+ Cervical Lesion Tissues

The results of RT<sup>2</sup> profiler PCR array confirmed that genes were differentially expressed < 2-fold (downregulation) and > 2-fold (upregulation) in the HSIL (hrHPV+, 14 cases) and CSCC (hrHPV+, 17cases) groups compared to normal control (NC) group, in order to investigate differentially expressed gene of innate and adaptive immune responses related to the microenvironment (receptors, regulatory genes, upstream and downstream effector genes) in HPV+ or HPV- cervical tissues described above (Table S2A). After comparison of pairs using the Qiagen tool website, the presented heatmap showed that CXCL10 was significantly overexpressed in CSCC, with a 3.02-fold increase in HSIL vs NC (*P* < 0.05), 35-fold in CSCC vs NC (*P* < 0.05) and a 12.21 fold increase in CSCC vs HSIL (*P* < 0.05) (Figures 1A, B and Table S2C). Moreover, upregulation of CXCL10 was confirmed in a second assay measuring gene expression of the TLR signaling pathway, which showed a 4.33-fold increase in HSIL vs NC and 47.42-fold in CSCC vs NC (Figures 1C, D and Table S2B). And qRT-PCR result

**TABLE 2** | Subtype distribution of high-risk HPV infection in different cervical lesions (n%).

Subtype of hrHPV infection	Normal control (20 cases)	HSIL (20 cases)	CC (20 cases)
16	0	8 (40%)	13 (65%)
18	0	0	8 (40%)
31	0	3 (15%)	1 (5%)
33	0	1 (5%)	0
35	0	0	0
39	0	1 (5%)	1 (5%)
45	0	1 (5%)	1 (5%)
51	0	1 (5%)	0
52	0	4 (20%)	3 (15%)
56	0	0	0
58	0	0	0
59	0	1 (5%)	0
68	0	0	0

substantiated the high expression levels of CXCL10 in CSCC (Figure 1E).

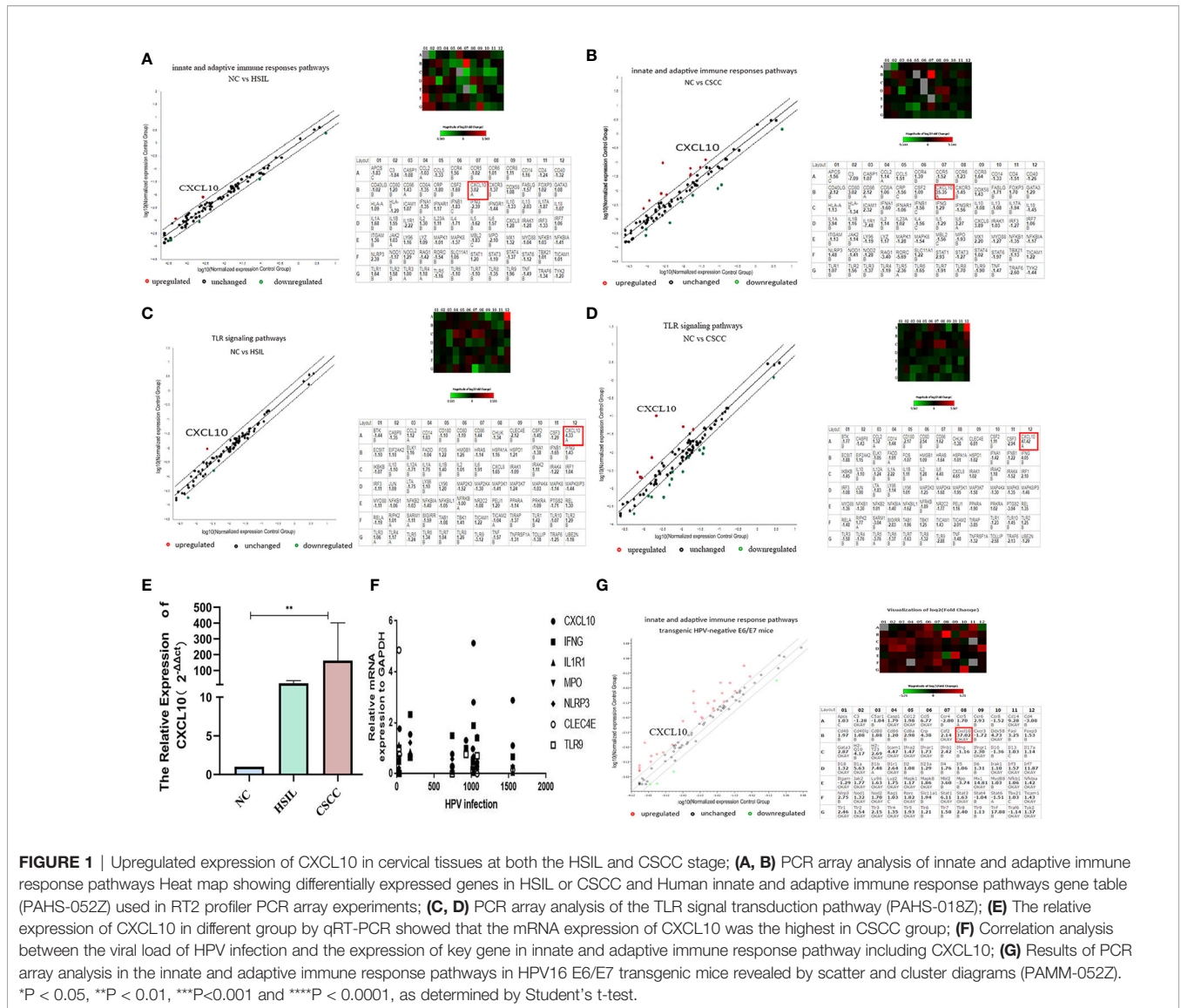
The correlations between the relative mRNA expression of differential genes from the PCR array analysis and quantitative titer of HPV infections were evaluated using the Spearman correlation test. Correlation analysis revealed that the viral load of HPV infection only had a statistically significant correlation for the expression of CXCL10 in innate and adaptive immune response signaling pathways (*r* = 0.662, *P* < 0.05). There was aggregation of gene expression in the concentration area of different HPV infections, which was just at the beginning of the infection stage (0 – 300), and 800 – 1,000, 1,500 and so on (Figure 1F).

### Upregulated CXCL10 Expression in the Innate and Adaptive Immune Responses in HPV16 E6/E7 Transgenic Mice

To investigate further whether CXCL10 in cervical cancer might be associated with epithelial atypical hyperplasia or carcinogenesis caused by HPV infection (29), HPV16 E6/E7 transgenic mice models, 8 founder lines, were established by breeding into C57BL/6×C57BL/6 hybrid mice. The tissues from the HPV16 E6/E7 transgenic mice were analyzed histologically to characterized consequences of E6 and E7 expression in cervix epithelia, which presented mild epidermal hyperplasia through HE staining (Figure S1C) and Immunohistochemistry (Figure S1D). Furthermore, cervix tissues from HPV E6/E7 transgenic mice and control groups were also detected with PCR array for innate and adaptive immune response pathways(QIAGEN, Cat. no. PAMM-052Z). Surprisingly, compared to normal mice, the

**TABLE 1** | HPV infection in 60 cases of cervical lesions.

Group	Cases	HPV (+)	HPV (-)	Multiple infections	Single infection	hrHPV infection	Low-risk HPV infection	HPV positive incidence
NC	20	2	18	0	2	0	2	10%
HSIL	20	17	3	4	13	14	3	85%
CSCC	20	20	0	1	19	17	3	100%
<i>P</i> -value								< 0.05



cervical tissues from HPV E6/E7 transgenic mice expressed a 37.23-fold increase in CXCL10 ( $P < 0.05$ ) (Figure 1G). In sum, our findings demonstrated significantly increased levels of CXCL10 by HPV-transformed cervical epithelium (Table S2). Notably, in the innate immune response pathway, IRF7 and MX1 were greatly increased, which act as IFN regulatory factors and as anti-myxovirus proteins. Others have shown that it was pivotal for the regulation of the IFN responses to evoke antiviral effect in innate immunity (30, 31).

### Elevated Secretion of CXCL10 in HPV+ CSCC Cells

To evaluate whether HPV infection was able to modulate the secretion of CXCL10 in HPV+ cells, KoE6/E7SiHa, a HPV E6/E7 knockout SiHa cell line was established through CRISPR/Cas9 gene editing and the knockout efficiency of the E6 and E7 gene by qPCR was 96.7% and 93.6%, respectively (Figures 2A, B). Actually, KoE6/E7 SiHa cells grew at a significantly slower rate

than SiHa cells *in vitro* through CCK-8 assay and Annexin V staining apoptosis assay, suggesting that the cell apoptosis induction and proliferation inhibition were markedly induced by the knockout of E6 and E7 (Figures S3A, B). CXCL10 expression was determined by western blotting of HFF-1 (HPV- human epithelial foreskin fibroblasts cells), H8 (HPV+, cervical immortalized cells), SiHa (HPV+, cervical cancer cells), KoE6/E7 SiHa (HPV-E6E7 knockout cells) and the results showed that the expression of CXCL10 was greater in HPV+ compared to HPV-cell lysates (Figure 2C). Next, to verify further whether HPV infection was responsible for higher CXCL10 secretion in HPV+ cells, the supernatants of cells including HFF-1, SiHa, Caski as well as KoE6/E7 SiHa cells were collected to detect the expression of CXCL10 using ELISA. The results demonstrated that the secretion of CXCL10 increased in HPV+ cells and decreased in the HPV-group (Figure 2D). In contrast, CXCR3, as the receptor of CXCL10, was expressed more abundantly in HPV- cells (Figure 2C). Surprisingly, the

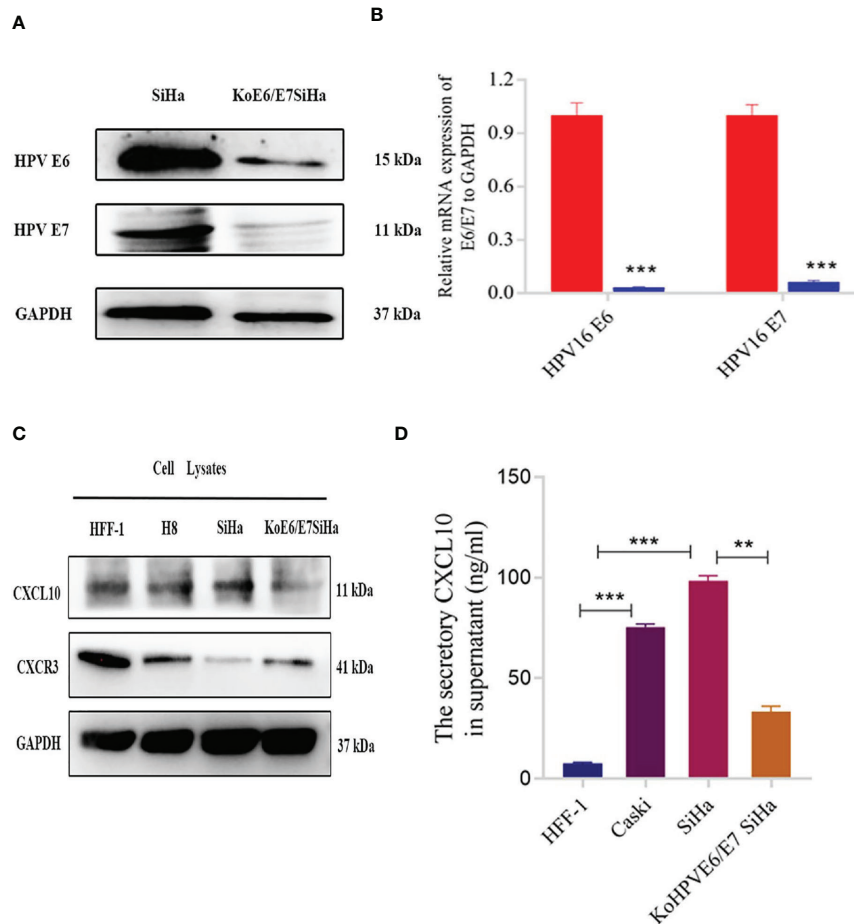


**FIGURE 2** | Expression of CXCL10 in different cells revealed by western blotting and Elisa. **(A, B)** The results of western blotting and qPCR verified that the KoE6/E7SiHa cell line was established successfully by CRISPR/Cas9 gene editing; **(C)** The expression of CXCL10 was tested through western blotting in different cell lines including HFF-1, H8, SiHa and KoE6/E7 SiHa; **(D)** The result of Elisa displayed increased secretion of CXCL10 in cervical cancer cells (SiHa and Caski), while was reverse in koE6/E7SiHa cell. \* $P < 0.05$ , \*\* $P < 0.01$ , \*\*\* $P < 0.001$  and \*\*\*\* $P < 0.0001$ , as determined by Student's t-test.

results indicated that CXCL10 was mainly expressed and secreted by HPV+ cells while CXCR3 was preponderant in HPV- cells (Figures 2C, D). Thus, we hypothesized that HPV+ cells might have a remarkable influence on HPV- cells through complex CXCL10-CXCR3 interactions.

## HPV-Mediated Expression of CXCL10 and Signaling *via* CXCR3 Induces PD-L1 Expression

It has been reported that HPV+ tumors tend to have an increased tumor-associated immune cell infiltrate relative to HPV- tumors (32, 33). However, the mechanisms responsible for these differences have not been fully elucidated. In the present study, a total of 25 specimens of cervical squamous cell carcinoma (CSCC) were collected from 14 HPV+ and 11 HPV- patients (Table S1). Immunohistochemistry revealed that in CSCC lesions, the expression of PD-L1 had a strong relationship with HPV infection (Figure 3A). *In vitro*, the expression of PD-L1

showed that upregulated expression of PD-L1 tended to occur mainly in HPV+ cells (Figure 3B).

Actually, this study showed a significantly increased production of multiple chemokines including CXCL10 in HPV+ specimens as well as in transgenic mice. It has been reported that CXCL9/10/11 is a regulator of PD-L1 expression in gastric cancer (14, 28). To explore whether the secretion of CXCL10 was responsible for the expression of PD-L1, a transwell co-culture assay was performed for 48 h using HFF-1 and KoE6/E7 SiHa cells. As shown in Figure 3B, after co-culture with HPV+ cells (SiHa, Caski), PD-L1 expression in HFF-1 was upregulated (Figures 3C, D). However, when the SiHa or Caski cells cultured in the chamber of a transwell were treated with 1  $\mu$ M AMG487, which prevents CXCL10-CXCR3 binding, the upregulation of PD-L1 was suppressed (Figures 3C, D). To confirm further the specific effect of CXCL10, recombinant human CXCL10 at a concentration of 100 ng/ml was directly added to the culture of HFF-1 and KoE6/E7 SiHa cells for 48 h, respectively and then treatment results after the application of 1



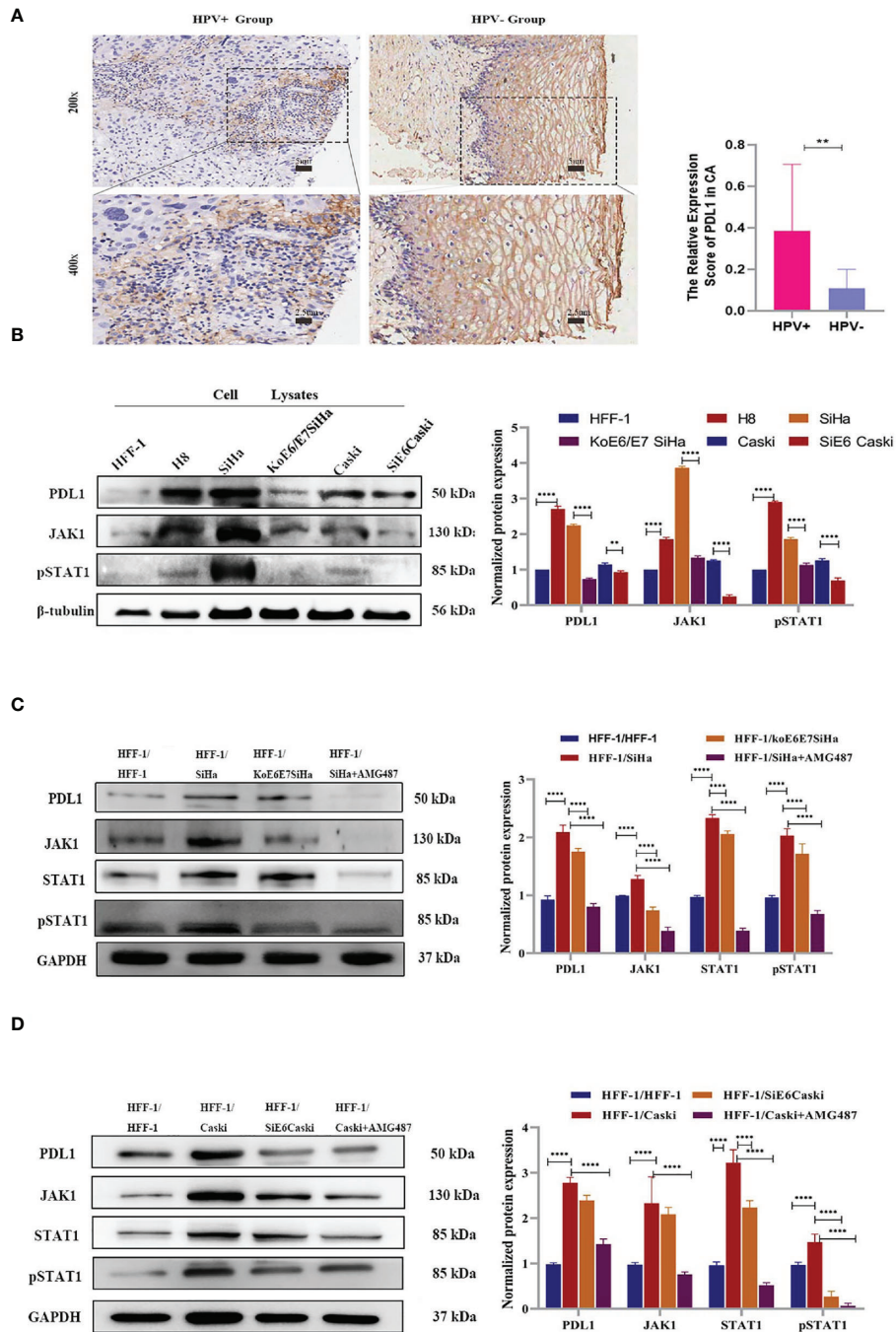


**FIGURE 3** | Through transwell co-culture with HPV+ cells (SiHa and Caski), PD-L1 expression in HFF-1 cells were induced by CXCL10-CXCR3 interaction, while were decreased after co-culture with the HPV+ cells which E6 and E7 has been knocked down or treatment with AMG487. **(A)** Immunohistochemistry revealed that the expression of PD-L1 had a strong relationship with HPV infection in cervix tissues, which showed the higher expression of PD-L1 in CSCC (HPV+ Group) than that of a normal cervical epithelium (HPV- Group); **(B)** The expression of PD-L1, JAK1 and pSTAT1 in different cells was tested by western blotting. The band intensities were calculated using the ImageJ software. GAPDH was used as an internal control for the total protein measurement. The ratio of the target gene to GAPDH was used to conduct the statistical analysis. **(C, D)** Compared to the co-culture with HFF-1 cells, the expression levels of PD-L1, JAK1 and pSTAT1 in HFF-1 cells were all upregulated following co-culture with HPV+ cells (SiHa, Caski) while the upregulation of JAK1 and pSTAT1 were diminished after co-culture with koE6/E7SiHa and SiE6Caski cells or treatment with AMG487 using the 0.4 μm polycarbonate membrane transwell assay, in which cells could not pass through. \*P < 0.05, \*\*P < 0.01, \*\*\*P < 0.001 and \*\*\*\*P < 0.0001, as determined by Student's t-test.

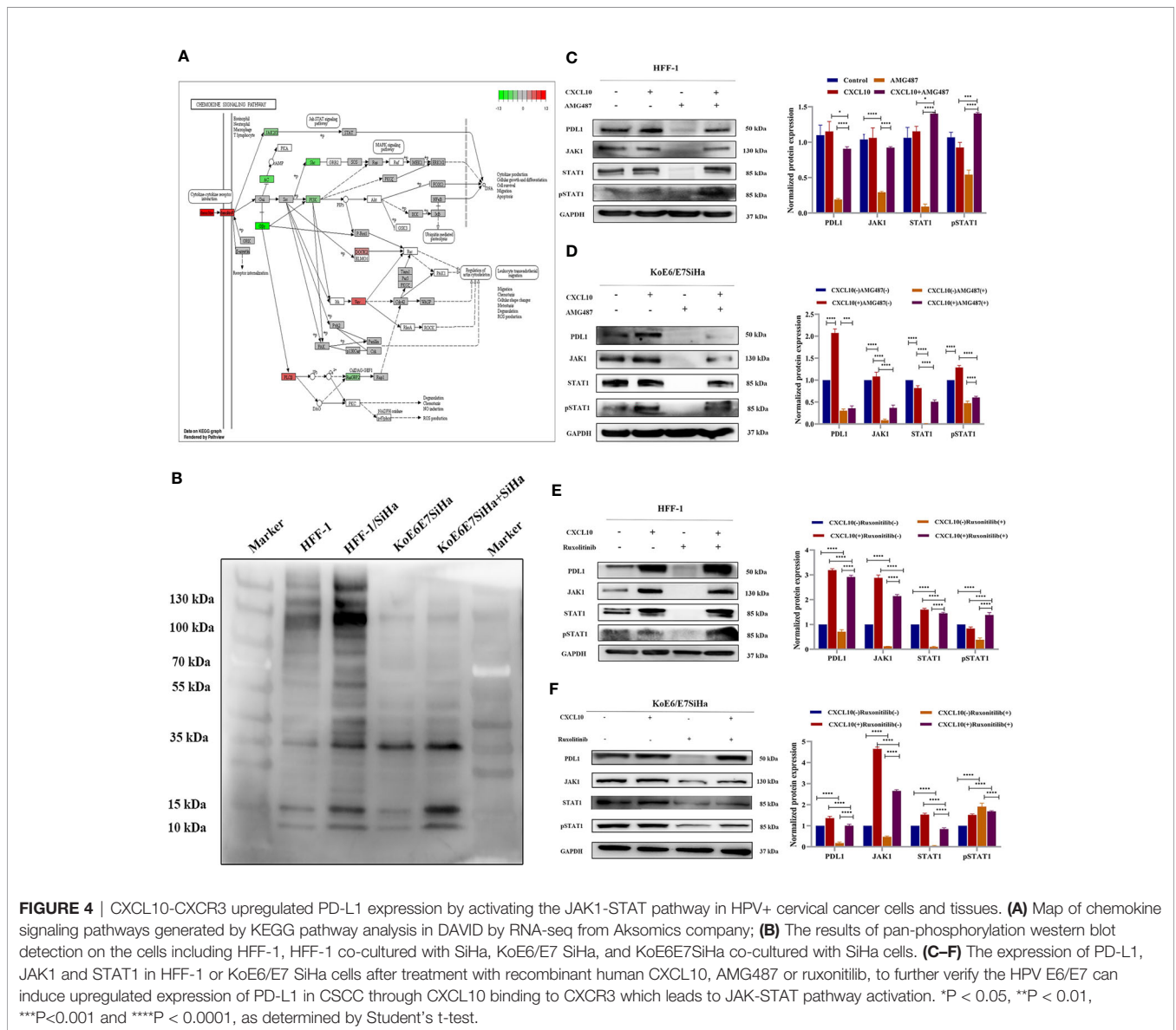
μM AMG487 were subsequently processed. The results showed that PD-L1 was upregulated by CXCL10 and downregulated after AMG487 treatment as expected, suggesting that HPV infection can induce PD-L1 expression by HPV+ cervical cancer through CXCL10-CXCR3 interactions.

### CXCL10 Secreted by HPV+ CSCC Cells Enhanced PD-L1 Expression by CXCL10-CXCR3 Activating the JAK1-STAT Pathway

According to the map of the KEGG pathway in the DAVID database, the JAK-STAT pathway acts as a downstream pathway for the chemokine-chemokine R downstream pathway (CXCL10-CXCR3) (Figure 4A). The difference of pan-phosphorylation among the cell lines including HFF-1, HFF-1 co-cultured with SiHa, KoE6/E7 SiHa, and KoE6E7SiHa co-cultured with SiHa cells revealed that the phosphorylated

proteins of the cells co-cultured with SiHa were significantly increased, which indicated that some proteins of the HPV- cells could be phosphorylated and activated by the key protein of HPV+ cells (Figure 4B) (34). Interestingly, the PCR array results showed that STAT1 was precisely overexpressed in CSCC vs the NC or HSIL groups ( $P < 0.05$ ). Therefore, we hypothesized that CXCL10 may regulate PD-L1 expression through the JAK-STAT pathway (Table S2).

In order to verify the JAK-STAT pathway, HFF-1 and KoE6/E7 SiHa cells were treated with recombinant human CXCL10. Notably, targeting JAK proteins or CXCR3 met with success in decreasing the expression of JAK1 and pSTAT1 after treatment with AMG487 (Figures 4C, D) and ruxonitililb (Figures 4E, F). Therefore, our findings demonstrated a correlation between suppression of STAT1 activation after JAK1 inhibition, evidenced by STAT phosphorylation, and downregulation of PD-L1. Moreover, the effect of the inhibitor on cells was reversed



by recombinant human CXCL10, suggesting that CXCL10-CXCR3 interaction play an important role in PD-L1 upregulation by activating the JAK1-STAT1 pathway in HPV- cells.

### PD-L1 Is Specifically Secreted and Transported by Exosomes in HPV+ CSCC

Interestingly, PD-L1 could not be directly detected in the cell supernatant, mentioned above, by ELISA. Our evidence has shown that PD-L1 existed in cell exosomes (Figure 5A) (Figure S2). Next, a tumor model was established by subcutaneous injection of  $5 \times 10^5$  SiHa or KoE6/E7 SiHa cells in 120  $\mu$ l of PBS into the flanks of nude mice (Figures S3C, D). After collecting the exosomes, the expression level of PD-L1 was higher in the SiHa group, followed by the KoE6/E7SiHa group,

a finding which implied that PD-L1 could be packaged into exosomes in CSCC (Figure 5B).

### DISCUSSION

Persistent HPV infection is involved in the pathogenesis of cervical cancer and is strongly associated with its prognosis (35). The oncogenic protein hrHPV E6/E7 may disrupt the regulation of gene expression in host cells that leads to abnormal cell proliferation by affecting the mechanisms involved in the control of the cell cycle and antigen presentation, rendering the body in a state of unresponsiveness (5, 35). Thus, tumor cells will evade attack by the immune system of the host and cancer immune surveillance, which is known as

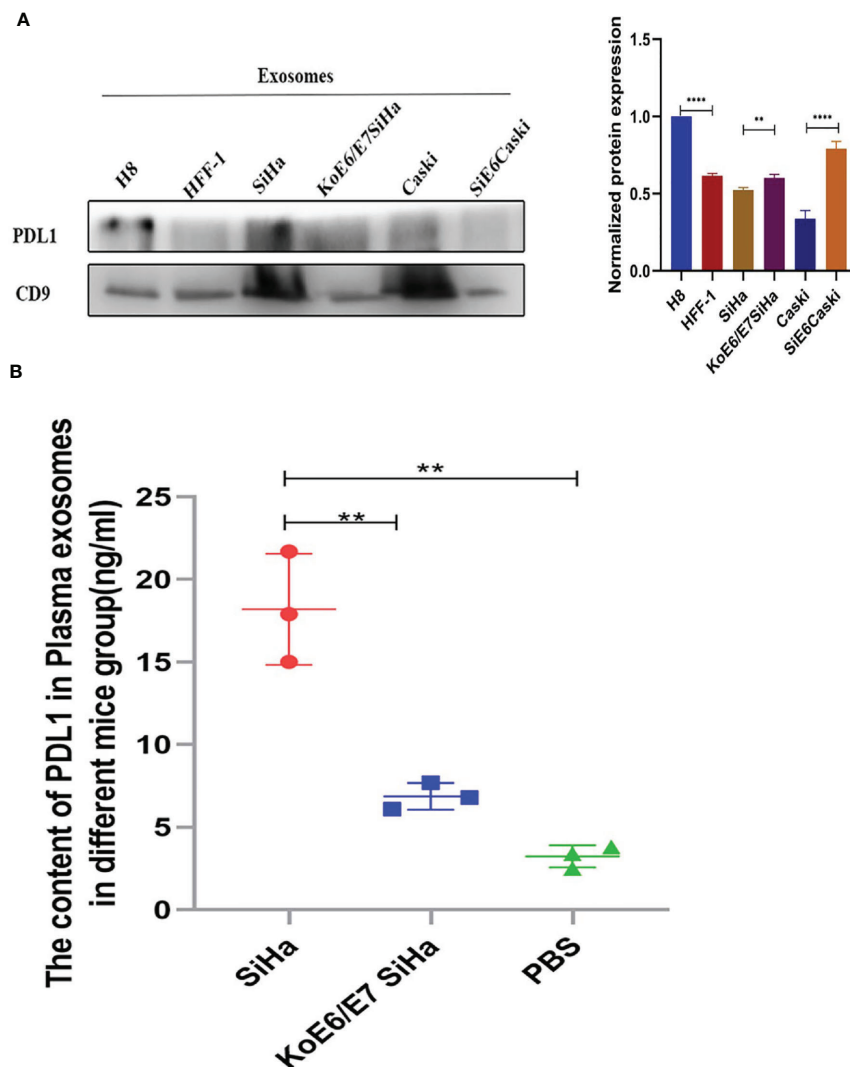


**FIGURE 5** | Expression levels of PD-L1 in the NC, SiHa and KoE6/E7 SiHa groups. **(A)** Western blotting showed that PD-L1 was present in cell exosomes; **(B)** ELISA revealed that the expression levels of exosomal PD-L1 was higher in the SiHa subcutaneous tumor group than that in KoE6/E7 SiHa, which were obtained by approximately 1 ml blood collected from the heart of mice from per mouse. \* $P < 0.05$ , \*\* $P < 0.01$ , \*\*\* $P < 0.001$  and \*\*\*\* $P < 0.0001$ , as determined by Student's t-test.

tumor immune escape, leading to the induction of tumorigenesis and progression (36). A number of investigators have proposed the cancer immunoediting hypothesis, namely that during tumor growth the microenvironment simultaneously aids tumor escape from immune surveillance (37). Several research groups have investigated whether HPV infection could affect PD-L1 expression in cervical cancer and reported that HPV positivity was positively correlated with increased PD-L1 expression (38, 39). This evidence indicates a potential role for PD-1/PD-L1 interactions in creating an “immune-privileged” site for initial HPV infection and subsequent adaptive immune resistance (40). Therefore, it is important to elucidate the regulatory mechanism between HPV infection and PD-L1. Our study showed that PD-L1 expression was enhanced by HPV infection *via* the chemokine subfamily CXCL10-CXCR3 axis in a JAK and STAT-dependent manner in CSCC cells, suggesting that chemokines may induce PD-L1 expression through JAK-STAT pathways.

The CXCL10 chemokine ligand 10, also known as IFN- $\gamma$ -inducible protein 10 (IP-10), is an IFN-induced protein having the ability to trigger lymphocyte chemotaxis (41). Previous studies have shown that CXCL10 has critical biological functions, such as selective expression of CXCR3 on Th1 cells and the regulation of immune cell migration, differentiation and activation (38, 41). CXCL10 has long been known to exert anti-malignancy functions by influencing the tumor microenvironment. Recently, some researchers have taken a different approach and investigated the direct effects of CXCL10 on tumor-promoting functions in colorectal carcinoma cells (42). The data supported the potential for CXCL10/CXCR3 co-expression as a predictor of metastatic recurrence (17). However, in the present study, the expression levels of CXCL10 in cervical lesions both in the HPV+ HSIL and CSCC groups as well as in HPV E6/E7 transgenic mice were significantly increased in the innate and adaptive signaling pathways. In addition, the secretion of CXCL10 was more apparent in HPV+ cervical cancer cells compared to non-infected and immortal epithelial cells. After dealing with SiHa cells by CRISPR/Cas9 gene editing, the E6/E7 knockout resulted in a major decrease of CXCL10 in KoE6/E7 SiHa, indicating a crucial function of HPV E6/E7 in the regulation of CXCL10 in human cervical cells as well.

Interestingly, our study found that PD-L1 was overexpressed in CSCC cells and CSCC tissues infected with HPV, especially in the exosome of CSCC cells as well as in the plasma of transplanted tumor mice. This novel HPV E6/E7-mediated mechanism of action may have developed to strengthen the secretion of the chemokine CXCL10 in the innate and adaptive immune response pathways. This allows the CXCL10-CXCR3 axis to upregulate PD-L1 expression by activating JAK and STAT pathways in fibroblasts to facilitate viral latency and avoidance of immune system viral attack. The finding is of significant interest to the field, challenging the paradigm that the effects of CXCL10 are anti-tumor immune responses (43) through immunosuppressive mechanisms, including upregulated expression of PD-L1.

## CONCLUSIONS

In summary, our results from data analysis and *in vitro* and *in vivo* experiments have suggested a regulatory mechanism of HPV infection-related upregulation of PD-L1, which is an important factor for immune evasion in HPV+ CSCC cells. CXCL10-CXCR3 may well regulate PD-L1 expression through JAK and STAT signaling pathways in fibroblasts cells. Checkpoint blockers such as PD-L1 offer novel immunotherapy options for cancer patients. Based on our findings, CXCL10-CXCR3 could be a potential target for CSCC therapy but further studies will be required to confirm this conjecture.

## DATA AVAILABILITY STATEMENT

The raw data supporting the conclusions of this article will be made available by the authors, without undue reservation.

## ETHICS STATEMENT

The animal study was reviewed and approved by Shenzhen Hospital, Southern Medical University.

## AUTHOR CONTRIBUTIONS

Conceived and designed the experiments: YH, XG, XL. Performed the experiments: XG, YX, XNC, MY. Analyzed the data: XG, XY and HH. Contributed reagents/materials/analysis tools: YH, XG, AH, JLY. Wrote the paper: XNC, XG, YX. Review and Editing: XNC, HH. All authors contributed to the article and approved the submitted version.

## FUNDING

This study was supported by the National Natural Science Foundation of China (No.81972423); the project of free exploration from Shenzhen Technology Innovation Committee (JCYJ20170307144103633, JCYJ20190814111801681, JCYJ20190814110207603); the clinical research start-up plan of Southern Medical University (Grant no. LC2016YM018); a grant from the Shenzhen Key Laboratory of Viral Oncology (ZDSYS201707311140430) and a grant from the Sanming Medical Project (SM201702). The funding parties had no influence on the study design, data collection, analysis or interpretation of the results.

## SUPPLEMENTARY MATERIAL

The Supplementary Material for this article can be found online at: <https://www.frontiersin.org/articles/10.3389/fonc.2021.629350/full#supplementary-material>

**Supplementary Figure 1** | The establishment of HPV E6e7 transgenic mice; **(A)** Diagram illustrating the vector map used to generate transgenic mice; **(B)** Verification of the HPV16 E6/E7 transgenic mice by PCR array; **(C, D)** The cervix

tissues from the normal mice (NC) and the HPV16 E6/E7 transgenic mice (Tg) were analyzed histologically through HE staining and Immunohistochemistry, and the result of the HPV16 E6/E7 transgenic mice presented Basal cells with large, deeply stained nucleus gently.

**Supplementary Figure 2 |** Identification of the exosomes by electron microscopy and markers; **(A)** The representative transmission electron microscopy image displaying the morphology and size of exosomes; Scale bars, 200 nm; **(B)** Result displaying the CD63 and CD9 (exosomal marker) immunoblot in H8 and SiHa cell lines.

**Supplementary Figure 3 |** The results of tumor model by subcutaneous injection of  $5 \times 10^5$  SiHa or KoE6/E7 SiHa cells into nude mice. **(A, B)** The proliferation and apoptosis of SiHa and KoE6/E7 SiHa cells were detected by CCK-8 assay and Annexin V staining apoptosis assay; **(C)** The volume of tumor was determined from caliper measurements of tumor length (L) and width (W) according to the formula  $L \times W^2/2$ ; **(D)** The histology of tumors were detected by HE staining and **(E)** The expression of HPV oncogenes E6 and E7 was determined by immunohistochemistry, which further presented the higher expression of E6 and E7 protein in SiHa group than that in koE6/E7SiHa group.

## REFERENCES

- Steinbach A, Riemer A. Immune Evasion Mechanisms of Human Papillomavirus: An Update. *Int J Cancer* (2018) 142:224–9. doi: 10.1002/ijc.31027
- Chen X, Han L, Wu X, Wei W, Wu L, Yi H, et al. Clinical Significance of CD163+ and CD68+ Tumor-Associated Macrophages in High-risk HPV-Related Cervical Cancer. *J Cancer* (2017) 8:3868–75. doi: 10.7150/jca.21444
- Smola S. Immunopathogenesis of HPV-Associated Cancers and Prospects for Immunotherapy. *Viruses* (2017) 9(9):254. doi: 10.3390/v9090254
- Zhu H, Chen X, Hu Y, Shi Z, Zhou Q, Zheng J, et al. Long Non-Coding RNA Expression Profile in Cervical Cancer Tissues. *Oncol Lett* (2017) 14:1379–86. doi: 10.3892/ol.2017.6319
- Zhang S, Liu F, Mao X, Huang J, Yang J, Yin X, et al. Elevation of miR-27b by HPV16 E7 Inhibits Ppary Expression and Promotes Proliferation and Invasion in Cervical Carcinoma Cells. *Int J Oncol* (2015) 47:1759–66. doi: 10.3892/ijo.2015.3162
- Conway M, Meyers C. Replication and Assembly of Human Papillomaviruses. *J Dental Res* (2009) 88:307–17. doi: 10.1177/0022034509333446
- Hoppe-Seyler K, Bossler F, Braun J, Herrmann A, Hoppe-Seyler F. The HPV E6/E7 Oncogenes: Key Factors for Viral Carcinogenesis and Therapeutic Targets. *Trends Microbiol* (2018) 26:158–68. doi: 10.1016/j.tim.2017.07.007
- Senba M, Mori N. Mechanisms of Virus Immune Evasion Lead to Development From Chronic Inflammation to Cancer Formation Associated With Human Papillomavirus Infection. *Oncol Rev* (2012) 6:e17. doi: 10.4081/oncol.2012.e17
- Zhou Q, Zhu K, Cheng H. Toll-Like Receptors in Human Papillomavirus Infection. *Archivum Immunologiae Et Therapiae Experimentalis* (2013) 61:203–15. doi: 10.1007/s00005-013-0220-7
- O'Brien P, Campo S. Evasion of Host Immunity Directed by Papillomavirus-Encoded Proteins. *Virus Res* (2002) 88(1-2):103–17. doi: 10.1016/S0168-1702(02)00123-5
- Kawai T, Akira S. Toll-Like Receptors and Their Crosstalk With Other Innate Receptors in Infection and Immunity. *Immunity* (2011) 34:637–50. doi: 10.1016/j.immuni.2011.05.006
- Kumar H, Kawai T, Akira S. Biochemical and Biophysical Research Communications Toll-Like Receptors and Innate Immunity. *Biochem Biophys Res Commun* (2009) 388:0–625. doi: 10.1016/j.bbrc.2009.08.062
- Qian G, Jian Z, Jia B, Liang C. CXCL7 Promotes Proliferation and Invasion of Cholangiocarcinoma Cells. *Oncol Rep* (2017) 37:1114–22. doi: 10.3892/or.2016.5312
- Zhang C, Li Z, Xu L, Che X, Wen T, Fan Y, et al. CXCL9/10/11, a Regulator of PD-L1 Expression in Gastric Cancer. *BMC Cancer* (2018) 18:462. doi: 10.1186/s12885-018-4384-8
- Datta D, Flaxenburg JA, Laxmanan S, Geehan C, Grimm M, Waagasser AM, et al. Ras-Induced Modulation of CXCL10 and Its Receptor Splice Variant CXCR3-B in MDA-MB-435 and MCF-7 Cells: Relevance for the Development of Human Breast Cancer. *Cancer Res* (2006) 66:9509–18. doi: 10.1158/0008-5472.CAN-05-4345
- Ejaeidi AA, Craft BS, Punekey LV, Lewis RE, Cruse JM. Hormone Receptor-Independent CXCL10 Production Is Associated With the Regulation of Cellular Factors Linked to Breast Cancer Progression and Metastasis. *Exp Mol Pathol* (2015) 99:163–72. doi: 10.1016/j.yexmp.2015.06.002
- Wightman SC, Uppal A, Pitroda SP, Ganai S, Burnette B, Stack M, et al. Oncogenic CXCL10 Signalling Drives Metastasis Development and Poor Clinical Outcome. *Br J Cancer* (2015) 113:327–35. doi: 10.1038/bjc.2015.193
- Ling CC, Ng KTP, Shao Y, Geng W, Xiao JW, Liu H, et al. Post-transplant Endothelial Progenitor Cell Mobilization Via CXCL10/CXCR3 Signaling Promotes Liver Tumor Growth. *J Hepatol* (2014) 60:103–9. doi: 10.1016/j.jhep.2013.08.017
- Man K, Shih KC, Ng K, Xiao JW, Guo DY, Sun C, et al. Molecular Signature Linked to Acute Phase Injury and Tumor Invasiveness in Small-for-Size Liver Grafts. *Ann Surg* (2010) 251:1154. doi: 10.1097/SLA.0b013e3181d96e3d
- Moriai S, Takahara M, Ogino T, Nagato T, Kishibe K, Ishii H, et al. Production of Interferon-(Gamma)-Inducible protein-10 and Its Role as an Autocrine Invasion Factor in Nasal Natural Killer/T-Cell Lymphoma Cells. *Clin Cancer Res* (2009) 15:6771–9. doi: 10.1158/1078-0432.CCR-09-1052
- Vinet J, Jong E, Boddeke H, Stanulovic V, Brouwer N, Granic I, et al. Expression of CXCL10 in Cultured Cortical Neurons. *J Neurochem* (2010) 112(3):703–14. doi: 10.1111/j.1471-4159.2009.06495.x
- Antonelli A, Ferrari SM, Fallahi P, Frascerra S, Piaggi S, Gelmini S, et al. Dysregulation of Secretion of CXC  $\alpha$ -Chemokine CXCL10 in Papillary Thyroid Cancer: Modulation by Peroxisome Proliferator-Activated Receptor- $\gamma$  Agonists. *Endocrine Related Cancer* (2009) 16:1299–311. doi: 10.1677/ERC-08-0337
- Duruisseaux M, Rabbe N, Antoine M, Vieira T, Poulot V, Cadranel J, et al. Pro-Tumoural CXCL10/CXCR3-A Autocrine Loop in Invasive Mucinous Lung Adenocarcinoma. *ERJ Open Res* (2017) 3:00047–2016. doi: 10.1183/23120541.00047-2016
- Flores RJ, Kelly AJ, Li Y, Nakka M, Barkauskas DA, Krailo. A Novel Prognostic Model for Osteosarcoma Using Circulating CXCL10 and FLT3LG. *Cancer* (2017) 123(1):144–54. doi: 10.1002/cncr.30272
- Wang J, Sun H, Zeng Q, Guo XJ, Dong ZY. HPV-Positive Status Associated With Inflamed Immune Microenvironment and Improved Response to Anti-PD-1 Therapy in Head and Neck Squamous Cell Carcinoma. *Sci Rep* (2019) 9(1):13404. doi: 10.1038/s41598-019-49771-0
- Jiang Y, Liao Y, He H, Xin Q, Tu Z, Kong S, et al. Foxm1 Directs Stat3 Expression Essential for Human Endometrial Stromal Decidualization. *Sci Rep* (2015) 5:13735. doi: 10.1038/srep13735
- Tavassoli FA, Devilee P. WHO Classification of Tumours. In: *Pathology and Genetics of Tumours of the Breast and Female Genital Organs* 3rd Ed. Lyon: IARC Press (2003) p. 113–263.
- Qian K, Zhang J, Lu J, Liu W, Yao X, Chen Q, et al. FAM172A Modulates Apoptosis and Proliferation of Colon Cancer Cells Via STAT1 Binding to its Promoter. *Oncol Rep* (2016) 35:1273–80. doi: 10.3892/or.2015.4485
- Kuo P, Tuong ZK, Teoh SM, Frazer IH, Mattarollo S, Leggatt GR. Hpv16e7 Induced Hyperplasia Promotes Cxcl9/10 Expression and Induces Cxcr3+ T Cell Migration to Skin. *J Invest Dermatol* (2017) 138(6):1348–59. doi: 10.1016/j.jid.2017.12.021
- Nigg PE, Pavlovic J. Oligomerization and GTP-Binding Requirements of MxA for Viral Target Recognition and Antiviral Activity Against Influenza A Virus. *J Biol Chem* (2015) 290(50):29893–906. doi: 10.1074/jbc.M115.681494
- Negishi H, Taniguchi T, Yanai H. The Interferon (IFN) Class of Cytokines and the IFN Regulatory Factor (IRF) Transcription Factor Family. *Cold Spring Harb Perspect Biol* (2017) 10(11):a028423. doi: 10.1101/cshperspect.a028423
- Lechner A, Schler H, Rothschild SI, Thelen M, Beutner D. Characterization of Tumor-Associated T-Lymphocyte Subsets and Immune Checkpoint Molecules in Head and Neck Squamous Cell Carcinoma. *Oncotarget* (2017) 8:44418–33. doi: 10.18632/oncotarget.17901
- Partlová S, Bouček J, Kloudová K, Lukešová E, Zábrodský M, Grega M, et al. Distinct Patterns of Intratumoral Immune Cell Infiltrates in Patients With

- HPV-Associated Compared to Non-Virally Induced Head and Neck Squamous Cell Carcinoma. *Oncoimmunology* (2015) 4(1):e965570. doi: 10.4161/21624011.2014.965570
34. Cañadas I, Thummalapalli R, Kim JK, Kitajima S, Jenkins RW, Christensen CL, et al. Tumor Innate Immunity Primed by Specific Interferon-Stimulated Endogenous Retroviruses. *Nat Med* (2018) 24(8):1143–50. doi: 10.1038/s41591-018-0116-5
  35. Wang Y, Yu YH, Shen K, Lin X, Xiang H. Cervical Cancer Screening and Analysis of Potential Risk Factors in 43,567 Women in Zhongshan, China. *Asian Pacific J Cancer Prev Apjcp* (2014) 15:671–6. doi: 10.7314/APJCP.2014.15.2.671
  36. Frazer IH. Tolerance or Immunity to a Tumor Antigen Expressed in Somatic Cells Can Be Determined by Systemic Proinflammatory Signals at the Time of First Antigen Exposure. *J Immunol* (2001) 167:6180. doi: 10.4049/jimmunol.167.11.6180
  37. Dunn GP, Bruce AT, Ikeda H, Old LJ, Schreiber RD. Cancer Immunoediting: From Immunosurveillance to Tumor Escape. *Nat Immunol* (2002) 3(11):991–8. doi: 10.1038/ni1102-991
  38. Mezache L, Paniccia B, Nyinawabera A, Nuovo GJ. Enhanced Expression of PD L1 in Cervical Intraepithelial Neoplasia and Cervical Cancers. *Modern Pathol Off J United States Can Acad Pathol Inc* (2015) 28(12):1594–602. doi: 10.1038/modpathol.2015.108
  39. Liu C, Lu J, Tian H, Du W, Zhao L, Feng J, et al. Increased Expression of PD-L1 by the Human Papillomavirus 16 E7 Oncoprotein Inhibits Anticancer Immunity. *Mol Med Rep* (2016) 15(4):1063–70. doi: 10.3892/mmr.2016.6073
  40. Franzen A, Vogt TJ, Müller T, Dietrich J, Schröck A, Golletz C, et al. Pd-L1 (CD274 ) and PD-L2 (PDCD1LG2) Promoter Methylation Is Associated With HPV Infection and Transcriptional Repression in Head and Neck Squamous Cell Carcinomas. *Oncotarget* (2018) 9:641–50. doi: 10.18632/oncotarget.23080
  41. Marra F, Tacke F. Roles for Chemokines in Liver Disease. *Gastroenterology* (2014) 147:577–94.e571. doi: 10.1053/j.gastro.2014.06.043
  42. Zipin-Roitman A, Meshel T, Sagi-Assif O, Shalmon B, Avivi C, Pfeffer RM, et al. Cxcl10 Promotes Invasion-Related Properties in Human Colorectal Carcinoma Cells. *Cancer Res* (2007) 67:3396. doi: 10.1158/0008-5472.CAN-06-3087
  43. Yang L, Chen P, Luo S, Li J, Kang L, Hu H, et al. Cxc-Chemokine-Ligand-10 Gene Therapy Efficiently Inhibits the Growth of Cervical Carcinoma on the Basis of Its Anti-Angiogenic and Antiviral Activity. *Biotechnol Appl Biochem* (2011) 53:209–16. doi: 10.1042/BA20090012

**Conflict of Interest:** The authors declare that the research was conducted in the absence of any commercial or financial relationships that could be construed as a potential conflict of interest.

**Publisher's Note:** All claims expressed in this article are solely those of the authors and do not necessarily represent those of their affiliated organizations, or those of the publisher, the editors and the reviewers. Any product that may be evaluated in this article, or claim that may be made by its manufacturer, is not guaranteed or endorsed by the publisher.

Copyright © 2021 Chen, He, Xiao, Hasim, Yuan, Ye, Li, Hao and Guo. This is an open-access article distributed under the terms of the Creative Commons Attribution License (CC BY). The use, distribution or reproduction in other forums is permitted, provided the original author(s) and the copyright owner(s) are credited and that the original publication in this journal is cited, in accordance with accepted academic practice. No use, distribution or reproduction is permitted which does not comply with these terms.